

# Potential Connection between the Australian Summer Monsoon Circulation and Summer Precipitation over Central China

HE Sheng-Ping<sup>1,2</sup>

<sup>1</sup> Climate Change Research Center, Institute of Atmospheric Physics, Chinese Academy of Sciences, Beijing 100029, China

<sup>2</sup> Nansen-Zhu International Research Centre, Institute of Atmospheric Physics, Chinese Academy of Sciences, Beijing 100029, China

Received 10 December 2014; revised 5 January 2015; accepted 19 January 2015; published 16 May 2015

**Abstract** This study investigated the connection between the Australian summer monsoon (ASM) and summer precipitation over central China. It was found that, following a weaker-than-normal ASM, the East Asian summer monsoon and western North Pacific subtropical high tend to be stronger, yielding anomalous northward moisture to be transported from the western Pacific to central China. Besides, anomalous upwelling motion emerges over 30–37.5°N, along 110°E. Consequently, significant positive summer precipitation anomalies are located over central China. Further analysis indicated that the boreal winter sea surface temperature (SST) in the Indian Ocean and South China Sea shows positive anomalies in association with a weaker-than-normal ASM. The Indian Ocean warming in boreal winter could persist into the following summer because of its own long memory, emanating a baroclinic Kelvin wave into the Pacific that triggers suppressed convection and an anomalous anticyclone. Besides, the abnormal SST signal in the South China Sea develops eastward with time because of local air-sea interaction, causing summer SST warming in the western Pacific. The SST warming can further affect East Asian atmospheric circulation and precipitation through its impact on convection.

**Keywords:** Australian summer monsoon, East Asian summer monsoon, precipitation

**Citation:** He, S.-P., 2015: Potential connection between the Australian summer monsoon circulation and summer precipitation over central China, *Atmos. Oceanic Sci. Lett.*, **8**, 120–126, doi:10.3878/AOSL20140091.

## 1 Introduction

As one of the world's most populated agricultural regions, China is influenced significantly by summer precipitation in terms of both its society and economy. One of the most prominent features of the precipitation pattern over East China is the belt-like distribution of the climatological and anomalous rainfall (Zhu et al., 2011). The major summer precipitation anomalies can be distinguished by the leading empirical orthogonal function rainfall pattern that has one major center located over the Yangtze River valley and two centers with opposite sign over northern and southern China (Nitta and Hu, 1996; Hsu and Lin, 2007), which is closely associated with the East Asian summer monsoon (EASM).

The mechanisms related to the summer precipitation anomaly over China have been investigated extensively. One of the most frequently cited mechanisms is the influence of the El Niño-Southern Oscillation (ENSO), in which above-normal summer rainfall over the Yangtze River valley is usually preceded by warm equatorial eastern Pacific sea surface temperature (SST) in the previous winter (Wang, 2002; Wu and Wang, 2002). The mechanism of a delayed influence of ENSO on East Asian summer precipitation refers to an anomalous Philippine Sea anticyclone developing rapidly in the boreal fall of an El Niño year, and persisting until the ensuing summer due to positive thermodynamic feedback between atmospheric Rossby waves and the underlying warm-pool ocean (Wang et al., 2000).

In recent years, the interaction between the atmospheric climate systems of the Northern Hemisphere and Southern Hemisphere has emerged as a hot topic (Fan and Wang, 2004; Sun et al., 2008). As the most dominant climate system in South Asia and the tropical Australian region, the Australian summer monsoon (ASM) has drawn particular attention. Zheng et al. (2014) suggested that a stronger ASM could enhance surface westerlies over the western tropical Pacific, which might in turn trigger the onset of El Niño. Consequently, an impact of the ASM on East Asian summer precipitation is possible, but the nature of such a relationship remains unresolved. Investigating this possibility was the main purpose of the present reported study.

## 2 Data and methods

The datasets used in this study included: (1) monthly mean data derived from the National Centers for Environmental Prediction/National Center for Atmospheric Research Reanalysis (Kalnay et al., 1996); (2) monthly mean Extended Reconstructed SST (Smith et al., 2008) and interpolated outgoing longwave radiation (Liebmann and Smith, 1996) obtained from the National Oceanic and Atmospheric Administration (NOAA); and (3) anomalous precipitation at a horizontal resolution of 2.5° × 2.5° (Chen et al., 2002) obtained from NOAA (<http://www.esrl.noaa.gov/psd/>).

Several climate indices were used to facilitate the analysis, including (1) the ASM index, defined as the area-averaged sea level pressure in the domain (35–25°S, 120–150°E), where the pressure shows significant positive anomalies in association with a weaker-than-normal

ASM (figure not shown); (2) the EASM index, as defined by Wang (2002) and Wang and Fan (1999), denoted as EASMI and EASM2 respectively; and (3) the Niño3.4 index, obtained from the National Weather Service Climate Prediction Center. The Australian summer and East Asian summer were considered as December–February (DJF) and June–August (JJA) respectively. To remove the possible influence of a trend on the linear relationship, all datasets and indices were detrended before analysis.

### 3 Correlation between the ASM and summer precipitation over central China

To explore the potential connection between the ASM and summer precipitation over central China, the correlation between the ASM index and summer precipitation over East China during 1979–2014 was calculated. As shown in Fig. 1a, significant positive correlation coefficients (CCs) are found over central China, and the CCs reach 0.5 in some regions. This implies that, following a

weaker ASM, the summer precipitation over central China tends to be more abundant. Considering the fact that above-normal summer rainfall over the Yangtze River valley is usually preceded by warm equatorial eastern Pacific SST in the previous winter (Wang, 2002; Wu and Wang, 2002), we wondered if the significant correlation presented in Fig. 1a might derive from the contribution of ENSO, and therefore analyzed the correlation between winter (DJF) Niño3.4 index and the following summer's precipitation during 1979–2014 (Fig. 1b). Even though the spatial distribution in Fig. 1b is similar to that in Fig. 1a, the magnitude of correlation is much smaller. Besides, the correlation between the ASM index and the summer precipitation over central China remains significant after excluding the linear impact of winter ENSO (Fig. 1c). The correlation coefficient between the central China summer precipitation index (area-averaged in the domain of  $(30\text{--}37.5^{\circ}\text{N}, 102.5\text{--}115^{\circ}\text{E})$ , denoted as PI) and ASM index is as high as 0.61.

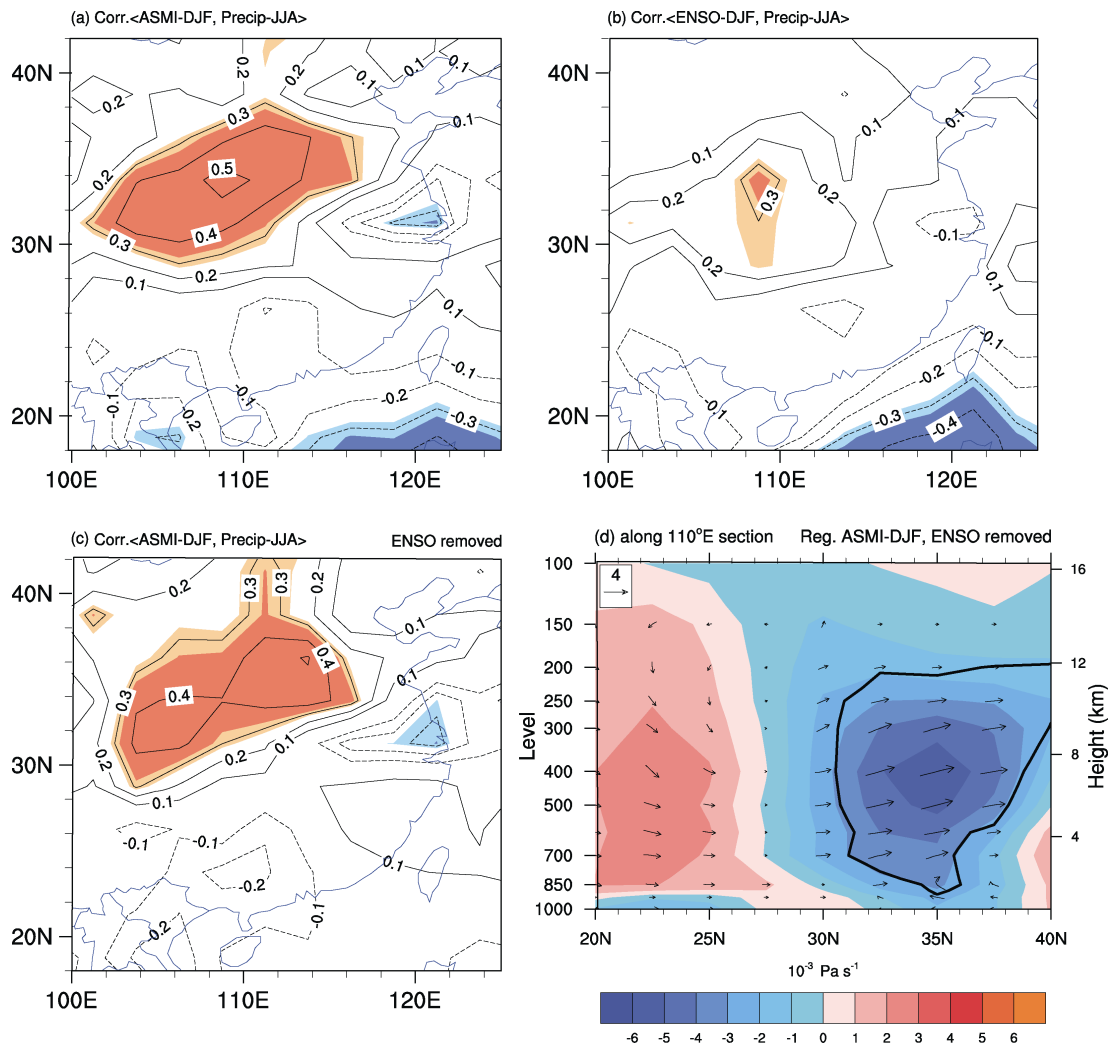


**Figure 1** Correlation between boreal summer (June–August, JJA) precipitation anomalies during 1979–2014 and (a) Australian summer monsoon index (ASMI) (December–February, DJF) and (b) preceding winter (DJF) Niño3.4 index. Light (blue and yellow) shading are at the 90% confidence level, and dark (blue and yellow) shading are at the 95% confidence level based on the Student's  $t$ -test. (c) As in (a), but with the signal of ENSO removed. (d) Vertical-horizontal cross section along  $110^{\circ}\text{E}$  for vertical wind (vectors; units:  $\text{m s}^{-1}$ ) and omega (shading, units:  $\times 10^{-3} \text{ Pa s}^{-1}$ ) anomalies during the summers of 1979–2014 regressed onto the ASMI (signal of winter ENSO removed). Omega anomalies enclosed by thick contours are at the 90% confidence level based on the Student's  $t$ -test.

#### 4 Boreal summer atmospheric circulation anomaly related to ASM

The EASM and western North Pacific subtropical high (WNPSH) are two important subsystems of the Yangtze River summer precipitation anomaly (Tao and Chen, 1987). We examined the changes of the WNPSH associated with the ASM. To remove any artificial trends of the raised isobaric surface at middle and lower latitudes caused by global warming (Yang and Sun, 2003; Lu et al., 2008; Huang et al., 2014), the study focused on the eddy geopotential height. And to exclude the possible effect of ENSO, the partial correlation between the ASM index and summer 850 hPa eddy geopotential height anomalies is presented (Fig. 2b). Following a weaker-than-normal ASM, the 850 hPa heights in summer are significantly higher than normal in the western North Pacific, suggesting a strengthening of the WNPSH. Correspondingly, strengthened southerly anomalies span from the western North Pacific northward to central China (Gong and Ho, 2003). This implies that the EASM is stronger than normal when the preceding ASM is weaker. The CCs of the ASM index with EASM1 and EASM2 are 0.57 and  $-0.60$  respectively (Table 1). To measure the intensity of the WNPSH, a WNPSH index was calculated, defined as the area-averaged 850 hPa eddy geopotential height in the domain of ( $15\text{--}30^\circ\text{N}$ ,  $120\text{--}150^\circ\text{E}$ ) (Huang et al., 2014).

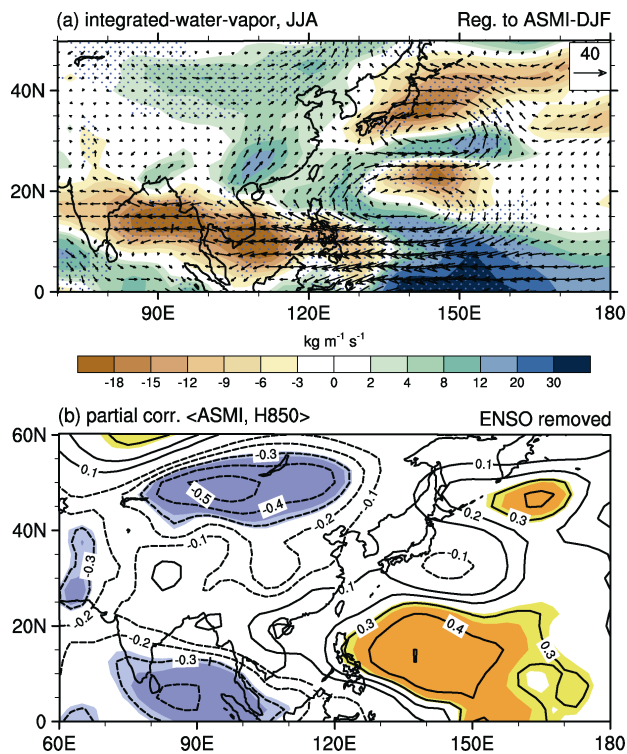


**Figure 2** (a) Regression map of vertically integrated (surface to 300 hPa) water vapor transport (vectors:  $\text{kg m}^{-1} \text{s}^{-1}$ ) and its magnitude (shading) during the summers of 1979–2014 with regard to the ASM. Dotted values indicate magnitude anomalies are statistically at the 90% confidence level based on the Student's *t*-test (signal of winter ENSO removed). (b) Partial correlation between the ASM and summer (JJA) 850 hPa eddy geopotential height anomalies, after removing the effects of ENSO. Light (blue and yellow) shading are at the 90% confidence level, and dark (blue and yellow) shading are at the 95% confidence level.

**Table 1** Correlation coefficients between indices. Further details regarding the Australian summer monsoon (ASM) and Niño3.4 indices can be found in section 2. EASM1 and EASM2 represent the East Asian summer monsoon (EASM) indices defined by Wang (2002) and Wang and Fan (1999). Further details regarding the central China summer precipitation index (PI) and the western North Pacific subtropical high (WNPSH) indices can be found in sections 3 and 4 respectively. Bold and italic values are at the 95% and 90% confidence levels respectively, based on the Student's *t*-test. DJF stands for December–February.

	EASM1	EASM2	PI	WNPSH
ASM (DJF)	<b>0.57</b>	<b><i>-0.60</i></b>	<b>0.61</b>	<b>0.56</b>
Niño3.4 (DJF)	<b>0.56</b>	<b><i>-0.59</i></b>	<b>0.34</b>	<b>0.50</b>
ASM <sup>1</sup> (DJF)	<i>0.29</i>	<i>-0.30</i>	<b>0.56</b>	<b>0.33</b>
Niño3.4 <sup>2</sup> (DJF)	0.27	<i>-0.30</i>	<i>-0.18</i>	0.17

<sup>1</sup>The linear signal of ENSO in the ASM index was removed

<sup>2</sup>The linear signal of the ASM in the Niño3.4 index was removed.

For the period 1979–2014, the correlation coefficient between the ASM and WNPSH indices is 0.56. Previous studies (Gong and Ho, 2003; Gong et al., 2011) have revealed that when the WNPSH intensifies or moves southward or extends westward, above-normal precipitation is expected to occur along the Yangtze River. Therefore, the changes of summer WNPSH related to the ASM could well explain the summer precipitation anomaly over central China. Given that the WNPSH plays an important role in modulating moisture transport over East Asia, vertically integrated (from the surface to 300 hPa) water vapor transport vector anomalies in summer for the period 1979–2014 was regressed onto the preceding ASM index, with the possible effect of winter ENSO having been removed (Fig. 2a). Generally speaking, the vertically integrated water vapor content over East China in summer is transported mainly from the tropical western Pacific and Indian Ocean, but the amount of water vapor transported from the Indian Ocean is comparatively larger (Wang and Chen, 2012). Consistent with the changes of EASM and summer WNPSH, the water vapor transported from the tropical western North Pacific is enhanced, though that transported from the Indian Ocean is weakened (Fig. 2a). The anomalous southerly water vapor extends from the South China Sea northward to central China. As a result, the air humidity over central China (including the Yangtze River) increases significantly (Fig. 2a). The center of the water vapor anomaly is located over central China (around  $30\text{--}45^\circ\text{N}$ ), which is consistent with the location of the summer precipitation anomaly (Figs. 1a and 1c).

In addition to moisture, vertical motion also plays an important role in inducing precipitation anomalies. Therefore, the change of summer vertical motion associated with the ASM was further examined. Unsurprisingly, following a weaker-than-normal ASM, there is anomalous upward motion over  $30\text{--}37.5^\circ\text{N}$ , along  $110^\circ\text{E}$  (Fig. 1d), which corresponds well to the location of the positive summer precipitation anomaly (Figs. 1a and 1c). Besides, there are southerly winds from the lower to the upper levels of the troposphere (Fig. 1d), suggesting a strengthened EASM.

In summary, in association with a weaker-than-normal ASM, the EASM and summer WNPSH are stronger, leading to an increase of water vapor content over central

China. Meanwhile, there is significant anomalous upward motion over 30–37.5°N, along 110°E. As a result, significant positive summer precipitation anomalies emerge over central China.

## 5 Possible mechanisms for the linkage

The question arises as to how the atmospheric anomalies and precipitation in summer over central China become established following a weaker ASM in the preceding boreal winter. To answer this question, the atmospheric circulation and SST anomalies over the Indian Ocean and

western Pacific were investigated, with the seasons of analysis extending from summer (JJA) back to the preceding winter (DJF). During winter, when the ASM is weaker than normal, an anomalous anticyclone is prominent at 850 hPa in Northwest Australia (between 90°E and 150°E, in the subtropical Southern Hemisphere), and another one is located over the Philippine Sea (Fig. 3a). Associated with the atmospheric circulation, there are also well-defined patterns in SST anomalies. There are basin-scale positive SST anomalies in the Indian Ocean and South China Sea, and at the same time significant negative

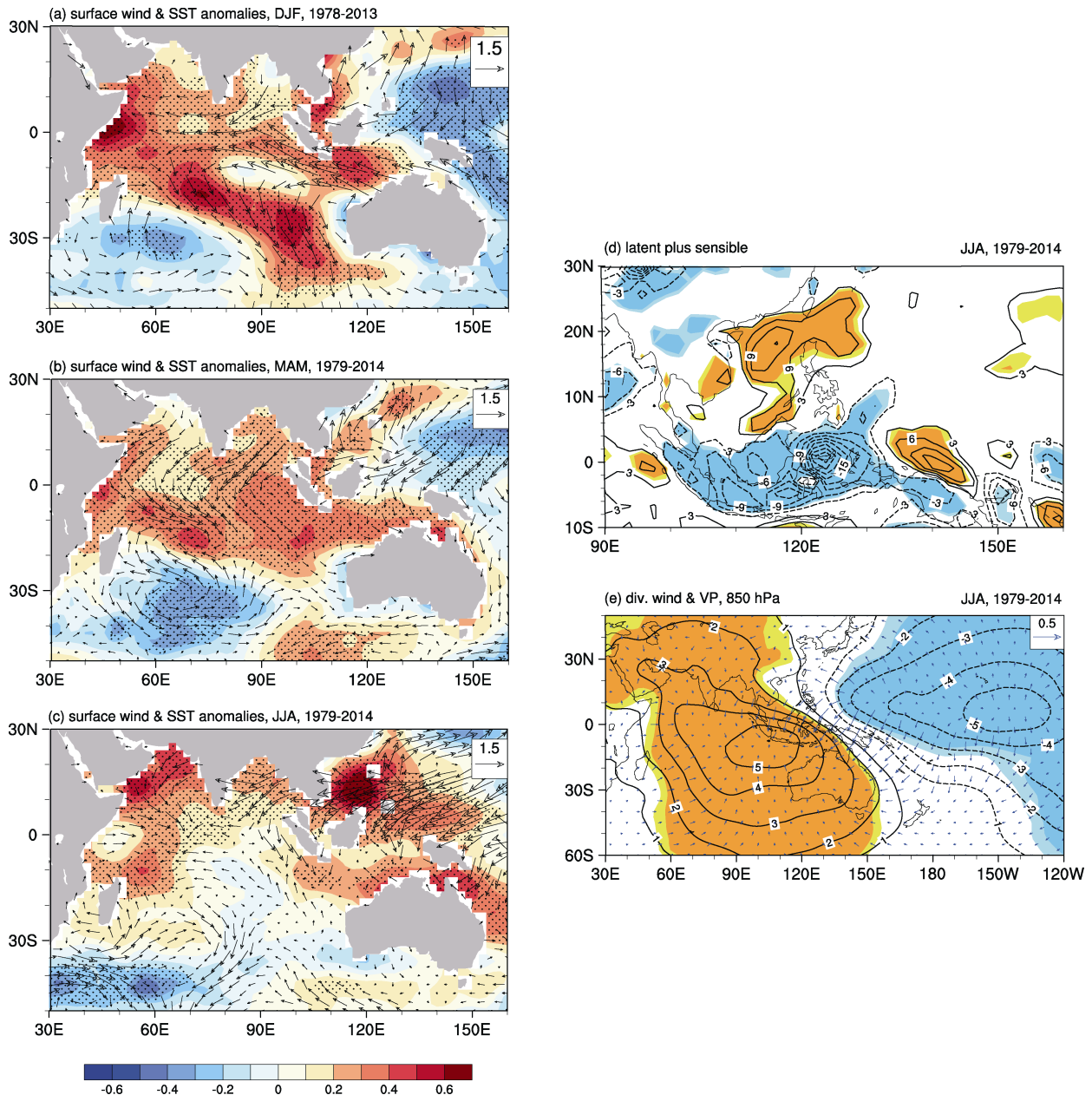


**Figure 3** Composite maps of the (a) DJF, (b) March–May (MAM), and (c) JJA surface wind (vectors; units:  $\text{m s}^{-1}$ ) and sea surface temperature (shading; unit:  $^{\circ}\text{C}$ ) anomalies (SSTAs) between high ( $\geq 0.5$  standard deviation) and low ( $\leq -0.5$  standard deviation) ASMI years during 1978–2013/1979–2014. The SST enclosed by the dotted regions is at the 90% confidence level based on the Student's *t*-test. Regression maps of summer (d) turbulent heat flux (contours, latent plus sensible; units:  $\text{W m}^{-2}$ ) and (e) the 850 hPa divergence component of the wind (vectors; scale in  $\text{m s}^{-1}$ ) and velocity potential (contours,  $10^5 \text{ m}^2 \text{ s}^{-1}$ ) during the summers of 1979–2014 with regard to the SSTA averaged in the domain of ( $0^{\circ}$ – $20^{\circ}\text{N}$ ,  $110^{\circ}$ – $150^{\circ}\text{E}$ ). Light (blue and yellow) shading are at the 90% confidence level, and dark (blue and yellow) shading are at the 95% confidence level.

SST anomalies are located in the tropical western Pacific (Fig. 3a). Note that, in association with the anomalous anticyclone in Northwest Australia, significant anomalous southerly winds extend northwestward from Australia, straight to the western North Indian Ocean, and then turn southeastward toward West Australia. The direction of the anomalous wind flow is highly consistent with the gradient of SST anomalies in the Indian Ocean. These features imply that the ASM-related atmospheric circulation anomalies play an essential role in producing the SST anomalies in the Indian Ocean. For the following two seasons, the SST anomalies show two pronounced features: one is that the SST signals in the Indian Ocean decrease gradually from winter through summer, and the other is the development and propagation of the South China Sea SST. In winter, there are significant positive SST anomalies in the South China Sea. Afterwards, these anomalies move eastward and lie over the western Pacific in the following summer (Fig. 3c).

Therefore, the connection between the ASM and summer precipitation over central China might be sustained in two ways. The Indian Ocean warming anomaly in winter could persist until the following summer because of its own long memory. According to Xie et al. (2009), the Indian Ocean warming acts like a capacitor, anchoring atmospheric anomalies over the Indo-western Pacific Ocean. It causes tropospheric temperature to increase by a moist-adiabatic adjustment in deep convection, emanating a baroclinic Kelvin wave into the Pacific. In the northwest Pacific, this equatorial Kelvin wave induces divergence in

the subtropics, which triggers suppressed convection and the anomalous anticyclone. On the other hand, the SST warming in the western Pacific can change spring surface winds (Zhou, 2011). Due to the increasing amplitude of the SST south of the equator being larger than that north of the equator, there is an obvious south-to-north SST difference across the equator over the Maritime Continent (Fig. 3b), leading to a southward sea level pressure gradient and the emergence of northerly winds. The Coriolis force turns these northerlies westward (eastward) to form northeasterlies (northwesterlies) north (south) of the equator (Fig. 3b). The northeasterly wind anomaly north of the equator opposes the mean southwesterly winds over the Maritime Continent and thus reduces evaporation and increases coastal downwelling, further warming the local SST (Fig. 3c). The summer SST warming can in turn affect the atmospheric circulation by air-sea interaction, as demonstrated by the summer turbulent heat flux anomalies associated with the simultaneous SST anomaly in the domain ( $0^{\circ}$ – $20^{\circ}$ N,  $110^{\circ}$ – $150^{\circ}$ E) (Fig. 3d). It is clear that the atmosphere obtains surface heat flux (negative anomalies) from the ocean over the Maritime Continent, which induces deep convection in the region (Fig. 3e). Meanwhile, significant surface divergence is dominant over the western North Pacific (Fig. 3e). The atmospheric response to western Pacific SST warming provides the dynamical conditions for the summer precipitation anomaly over central China.

The above mechanism is supported by the results presented in Fig. 4. Following a weaker-than-normal ASM,

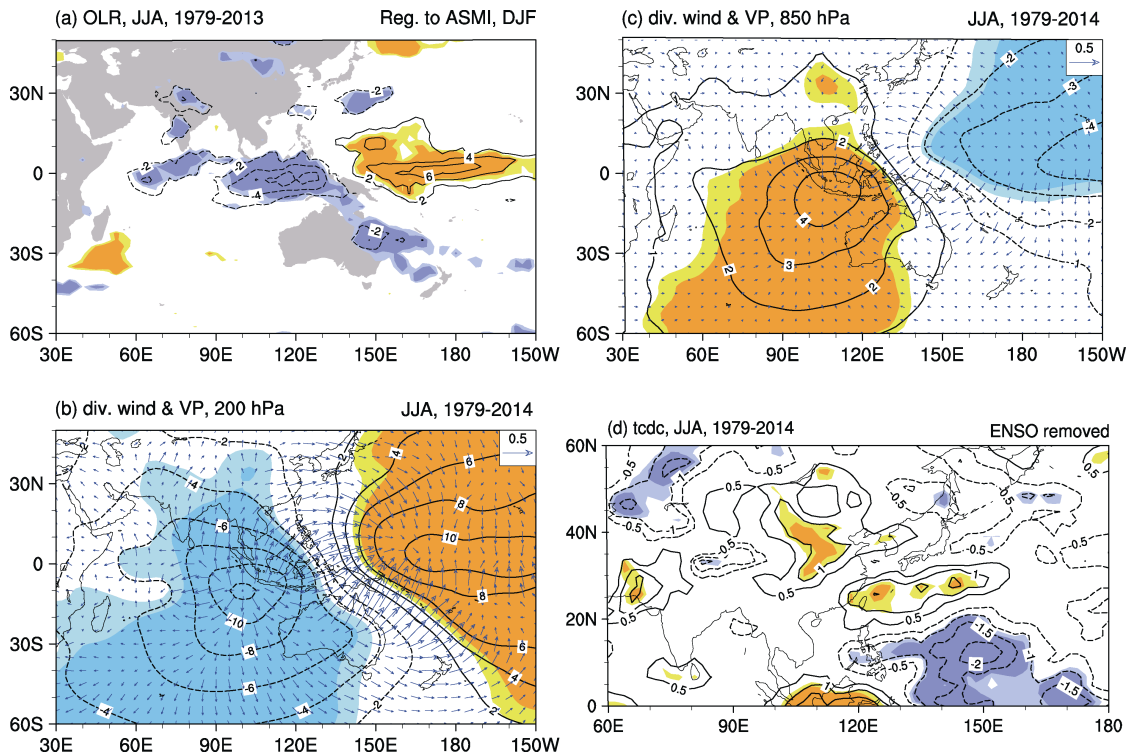


**Figure 4** Regression maps of (a) outgoing longwave radiation (OLR) (contours; units:  $W s^{-2}$ ; data only available to December 2013) and (b, c) the 200 and 850 hPa (respectively) divergence component of the wind (vectors; scale in  $m s^{-1}$ ) and velocity potential (contours;  $10^3 m^2 s^{-1}$ ), and (d) total cloud cover (units: %) during the summers of (a) 1979–2013 and (b, c, d) 1979–2014 with regard to the ASMI. Light (blue and yellow) shading are at the 90% confidence level, and dark (blue and yellow) shading are at the 95% confidence level, based on the Student's *t*-test (signal of winter ENSO removed).

there is a significant convection anomaly over the Maritime Continent and its western oceans during summer (Fig. 4a). Correspondingly, significant anomalous low-level tropospheric convergence/divergence (Fig. 4c) and upper tropospheric divergence/convergence (Fig. 4c) emerge over the Maritime Continent/western Pacific. The deep convection can extend northward to central China, which causes a significant positive total cloud cover anomaly in the region (Fig. 4d). Consequently, summer precipitation is more abundant than normal over central China.

## 6 Summary and discussion

The significant relationship between the ASM and summer precipitation over central China is supported by consistent changes in the EASM, summer WNPSH, and integrated water vapor content and vertical motion in East Asia during summer. Following a weaker-than-normal ASM, the EASM tends to be stronger. Meanwhile, an anomalous cyclonic circulation appears at 850 hPa in the western North Pacific during summer, yielding anomalous northward moisture transported from the western Pacific to central China. Besides, anomalous upwelling motion emerges over 30–37.5°N, along 110°E. Consequently, significant positive summer precipitation anomalies are located over central China.

The possible mechanism underpinning the link between the ASM and summer precipitation over central China was investigated with a focus on the seasonal atmospheric and oceanic changes associated with the anomalous ASM. Associated with a weaker-than-normal ASM, the boreal winter SST shows positive anomalies in the Indian Ocean and South China Sea. The Indian Ocean warming in boreal winter could persist to the following summer because of its own long memory, emanating a baroclinic Kelvin wave into the Pacific that triggers suppressed convection and an anomalous anticyclone (Xie et al., 2009). Besides, the abnormal SST signal in the South China Sea develops eastward with time because of local air-sea interaction, causing summer SST warming in the western Pacific. The SST warming can further affect East Asian atmospheric circulation and precipitation through its impact on convection. Importantly, similar results were obtained when another ASM index was adopted, defined as the area-averaged 850 hPa zonal wind over (15–5°S, 100–150°E) (Zhang and Zhang, 2010), suggesting a robust relationship between the ASM and summer precipitation over central China.

As revealed in many previous studies, above-normal summer rainfall over the Yangtze River valley is usually preceded by a warm equatorial eastern Pacific SST in the previous winter (Wu and Wang, 2002). Furthermore, the correlation coefficients between winter Niño3.4 index and the EASM1, EASM2, PI, and WNPSH indices are 0.56, –0.59, 0.34, and 0.50 respectively (Table 1). This means that the impact of ENSO cannot be ignored when discussing the connection between the ASM and EASM. On the other hand, the ASM might have its own independent impact on the EASM. For example, the correlation between the ASM and the EASM circulation, such as wind,

WNPSH (Table 1), and summer precipitation over central China (Fig. 1c), remain significant when the linear influence of ENSO has been removed. By contrast, the connection between ENSO and the summer WNPSH and summer precipitation over central China weakens dramatically after removing the effect of ASM on the EASM-related circulation and summer precipitation over central China (Table 1). Consequently, the ASM might be very useful for predicting the EASM and summer precipitation over central China.

**Acknowledgements.** This research was supported by the National Natural Science Foundation of China (Grant Nos. 41421004 and 41130103) and the Special Fund for Public Welfare Industry (Meteorology) (Grant No. GYHY201306026).

## References

- Chen, M., P. Xie, J. E. Janowiak, et al., 2002: Global land precipitation: A 50-yr monthly analysis based on gauge observations, *J. Hydrometeorol.*, **3**, 249–266.
- Fan, K., and H. J. Wang, 2004: Antarctic oscillation and the dust weather frequency in North China, *Geophys. Res. Lett.*, **31**, L10201, doi:10.1029/2004GL019465.
- Huang, Y. Y., H. J. Wang, K. Fan, et al., 2014: The western Pacific subtropical high after the 1970s: Westward or eastward shift? *Climate Dyn.*, doi:10.1007/s00382-014-2194-5.
- Hsu, H.-H., and S.-M. Lin, 2007: Asymmetry of the tripole rainfall pattern during the East Asian summer, *J. Climate*, **20**, 4443–4458.
- Gong, D.-Y., and C. H. Ho, 2003: Arctic oscillation signals in the East Asian summer monsoon, *J. Geophys. Res.*, **108**, 4066, doi:10.1029/2002JD002193, D2.
- Gong, D.-Y., J. Yang, S.-J. Kim, et al., 2011: Spring Arctic Oscillation-East Asian summer monsoon connection through circulation changes over the western North Pacific, *Climate Dyn.*, **37**, 2199–2216.
- Kalnay, E., M. Kanamitsu, R. Kistler, et al., 1996: The NCEP/NCAR 40-year reanalysis project, *Bull. Amer. Meteor. Soc.*, **77**, 437–471.
- Liebmann, B., and C. A. Smith, 1996: Description of a complete (interpolated) outgoing longwave radiation dataset, *Bull. Amer. Meteor. Soc.*, **77**, 1275–1277.
- Lu, R., Y. Li, and C. S. Ryu, 2008: Relationship between the zonal displacement of the western Pacific subtropical high and the dominant modes of low-tropospheric circulation in summer, *Prog. Nat. Sci.*, **18**, 161–165.
- Nitta, T., and Z.-Z. Hu, 1996: Summer climate variability in China and its association with 500 hPa height and tropical convection, *J. Meteor. Soc. Japan*, **74**, 425–445.
- Smith, T. M., R. W. Reynolds, T. C. Peterson, et al., 2008: Improvements to NOAA's historical merged land-ocean surface temperature analysis (1880–2006), *J. Climate*, **21**, 2283–2296.
- Sun, J. Q., J. H. Wang, and W. Yuan, 2008: A possible mechanism for the co-variability of the boreal spring Antarctic Oscillation and the Yangtze River valley summer rainfall, *Int. J. Climatol.*, **29**, 1276–1284.
- Tao, S. Y., and L. X. Chen, 1987: A review of recent research on the East Asian summer monsoon in China, in: *Monsoon Meteorology*, C.-P. Chang and T. N. Krishnamurti (Eds.), Oxford University Press, Oxford, 60–92.
- Wang, B., and Z. Fan, 1999: Choice of South Asian summer monsoon indices, *Bull. Amer. Meteor. Soc.*, **80**, 629–638.
- Wang, B., R. Wu, and X. Fu, 2000: Pacific-east Asian teleconnection: How does ENSO affect east Asian climate? *J. Climate*, **13**, 1517–1536.
- Wang, H. J., 2002: The instability of the East Asian summer mon-

- soon-ENSO relations, *Adv. Atmos. Sci.*, **19**, 1–11.
- Wang, H. J., and H. P. Chen, 2012: Climate control for southeastern China moisture and precipitation: Indian or East Asian monsoon? *J. Geophys. Res.*, **117**, D12109, doi:10.1029/2012JD017734.
- Wu, R., and B. Wang, 2002: A contrast of the East Asian Summer Monsoon-ENSO relationship between 1962–77 and 1978–93, *J. Climate*, **15**, 3266–3279.
- Xie, S. P., K. Hu, J. Hafner, et al., 2009: Indian Ocean capacitor effect on Indo-western Pacific climate during the summer following El Niño, *J. Climate*, **22**, 730–747.
- Yang, H., and S. Sun, 2003: Longitudinal displacement of the subtropical high in the western Pacific in summer and its influence, *Adv. Atmos. Sci.*, **20**, 921–933.
- Zhang, C., and H. Zhang, 2010: Potential impacts of East Asian winter monsoon on climate variability and predictability in the Australian summer monsoon region, *Theor. Appl. Climatol.*, **101**, 161–177.
- Zheng, Y., R. Zhang, and M. A. Bourassa, 2014: Impact of East Asian winter and Australian summer monsoons on the enhanced surface westerlies over the western tropical Pacific ocean preceding the El Niño onset, *J. Climate*, **27**, 1928–1944.
- Zhou, B. T., 2011: Linkage between winter sea surface temperature east of Australia and summer precipitation in the Yangtze River valley and a possible physical mechanism, *Chin. Sci. Bull.*, **56**(17), 1821–1827.
- Zhu, Y., H. Wang, W. Zhou, et al., 2011: Recent changes in the summer precipitation pattern in East China and the background circulation, *Climate Dyn.*, **36**, 1463–1473.